



# City Research Online

## City, University of London Institutional Repository

---

**Citation:** Basha, N., Kovacevic, A. ORCID: 0000-0002-8732-2242 and Rane, S. (2019). User defined nodal displacement of numerical mesh for analysis of screw machines in FLUENT. IOP Conference Series: Materials Science and Engineering, 604(1), doi: 10.1088/1757-899X/604/1/012012

This is the published version of the paper.

This version of the publication may differ from the final published version.

---

**Permanent repository link:** <http://openaccess.city.ac.uk/id/eprint/23227/>

**Link to published version:** <http://dx.doi.org/10.1088/1757-899X/604/1/012012>

**Copyright and reuse:** City Research Online aims to make research outputs of City, University of London available to a wider audience. Copyright and Moral Rights remain with the author(s) and/or copyright holders. URLs from City Research Online may be freely distributed and linked to.

---

City Research Online:

<http://openaccess.city.ac.uk/>

[publications@city.ac.uk](mailto:publications@city.ac.uk)

---

PAPER • OPEN ACCESS

## User defined nodal displacement of numerical mesh for analysis of screw machines in FLUENT

To cite this article: N Basha *et al* 2019 *IOP Conf. Ser.: Mater. Sci. Eng.* **604** 012012

View the [article online](#) for updates and enhancements.



**IOP | ebooks™**

Bringing you innovative digital publishing with leading voices to create your essential collection of books in STEM research.

Start exploring the collection - download the first chapter of every title for free.

# User defined nodal displacement of numerical mesh for analysis of screw machines in FLUENT

N Basha<sup>1</sup>, A Kovacevic<sup>1</sup> and S Rane<sup>2</sup>

<sup>1</sup>City, University of London, UK

<sup>2</sup>University of Oxford, Oxford, UK

E-mail: [Nausheen.basha@city.ac.uk](mailto:Nausheen.basha@city.ac.uk)

**Abstract.** Growing demands to reduce energy consumption are driving researchers towards in-depth analysis of positive displacement machines. Twin screw compressors are amongst the most common types of positive displacement machines. These machines have inherently complex geometry due to intricate rotor profiles used. As the details of the internal flows are difficult to obtain experimentally, Computational Fluid Dynamics (CFD) offers a good alternative for evaluation of internal flow patterns. However, implementation of CFD is challenging due to complex deforming geometries.

In this paper, a customised grid generator SCORG<sup>TM</sup> developed by authors is used to generate numerical meshes for commercially available solver ANSYS FLUENT. FLUENT is an unstructured solver which offers flexibility of using both segregated and coupled solution algorithms. Segregated algorithms are generally faster which results in shorter product development time. Interface with FLUENT is implemented by performing User Defined Nodal Displacements (UDND) of grids generated by SCORG in a parallel framework. For this purpose, SCORG and UDND are coupled and extended to work with FLUENT's parallel architecture. The developed code is compiled within the solver. The oil free air screw compressor with 'N' profile rotors and 3/5 lobe combination is modelled for 8000 RPM and 6000 RPM. Finally, the predicted performance values with FLUENT are compared to previously calculated CFX predictions and experimental results. FLUENT requires shorter solution time to obtain same accuracy of CFX.

## 1. Introduction

Compressed air accounts for a mean 10% of the global industrial electric energy consumptions and this share may reach 20% if commercial and residential needs are included [1][2]. These machines are widely used in a number of sectors like oil and gas, refrigeration, processing or mining. Thus, even minor improvement of efficiency will substantially reduce the world CO<sub>2</sub> production.

The principles over which this machine functions has been published during the early years of 1960 [3], followed by more publications on the profile design in foreign languages. In many cases, twin screw compressors have replaced reciprocating compressors [4]. Not only screw compressor technology is popular and sustainable, the market is projected to grow at a compound annual growth rate (CAGR) of 6.62% from 2016-2021, to reach a market size of USD 11.01 Billion by 2021 [5]. With increasing



market for this technology, it is important to explore computational techniques that would give an insight to compressor performance which can help in design improvements. Thermodynamic chamber models are commonly used in design and analysis of twin screw compressors to predict initial performance [6][7]. Though these models tend to predict overall performance rather than complete flow and pressure characteristics within compressor, but they are still popular because of their close to instant solution time.

Computational Fluid Dynamics (CFD) has been gaining an increasing popularity as a tool for design improvement within screw compressors as experimental measurements with these machines is challenging due its complex and deforming geometry. Kovacevic [8] [9] [10] made a breakthrough in CFD modelling of screw machines by developing a methodology to produce block structured grids for deforming domains using algebraic grid generation. Based on this, a standalone programme SCORG (Screw Compressor Rotor Grid Generator) is developed to generate and supply a numerical mesh and relevant parameters to commercial CFD solvers. Not only the computational modelling methodology was established, also the modelling results were closer to experimental results which encouraged further research in this direction. Rane and Kovacevic applied numerical orthogonalisation and smoothing to grids generated by analytical transfinite interpolation and eliminated the non-conformal interface between the rotor domains resulting in a single domain structured grid for the rotors resulting in better solution accuracy [11].

CFD analysis of screw compressor has been majorly explored with ANSYS CFX [12][13]. In one study comparison is made between the results obtained from CFX and PumpLinx solver for an air compressor. It was seen that segregated solver PumpLinx predicts better flow than coupled solver CFX while vice-versa for indicated power prediction. Recently, attempts were made to solve for a simplified expander geometry with Openfoam. Nevertheless, it was reported that complexity of deforming domain posed a serious challenge leading to unrealistic values of pressure and temperature at unexpected regions [14].

In this paper, ANSYS FLUENT is explored which is an unstructured solver with options of both coupled and segregated algorithms. With multiple choices on solver algorithm (pressure-velocity coupling) gives an advantage on solution time as segregated solvers are faster. However, the accuracy of segregated solver with FLUENT needs to be checked. This is achieved by solving for air screw compressor with both solvers CFX and FLUENT for 8000 and 6000 RPM. Before solving, with unstructured cell-centred solvers like cell numbers are updated when mesh is loaded in FLUENT. For this reason, along with commercial grid generators User Defined Nodal Displacements (UDND) have to be used to transition the nodes with the time step. UDND code is achieved by writing User Defined Functions (UDF) combining it with the parallel architecture as screw compressor cases are computationally intensive.

## 2. Grid generation

Various types of grid generation techniques for Finite Volume Methods (FVM) like mesh smoothing, tetrahedral re-meshing, hexahedral layering, key-frame remeshing and User Defined Nodal Displacement (UDND) are available. Popularly used approach to model deforming domains in screw compressors is analytical grid generation explained by Kovacevic et. al [10] and this was further developed to achieve a conformal boundary. 3D mesh generated from conformal boundary map with 2D cross sections allows the domains of male and female rotor to be combined into a single rotor mesh along with a procedure on smoothly transitioning rack ensures stability and accuracy in flow calculation [15]. These techniques have been integrated into a software package named SCORG™.

Most of the commercial CFD solvers have developed their own tools that successfully allow to interface the solver and customised grids. CFX uses a Fortran interface called 'junction box routine' to exchange external meshes with the solver. Similarly STAR-CCM+ has a C++ library that works with the user defined vertex motion module to pass node locations to the solver at each time step. PumpLinx has a mesh deformation function that reads the external node file to update node positions in the solver.

Interface created with FLUENT using User Defined Functions (UDF) and Dynamic mesh technique is explained in the section below.

### 2.1 Motion of customised grids with FLUENT solver

UDND is used along with customised grid generators to create a set of grids representing nodal locations for each time step. These are done prior to numerical flow calculation to guarantee that there is conservation of space and equations ('Node Mapping'). With unstructured solver and cell-centred solvers like that of FLUENT, node numbers are updated when the mesh is loaded in solver. The study performed by Bianchi et.al [16], addressed analytical grid generation based on UDND and ensures conservation of intrinsic quantities by maintaining cell connectivity and structure.

UDND is modelled in FLUENT through 'Dynamic mesh' update and smoothing methods. When smoothing is used to adjust the mesh motion of a zone with a moving or deforming boundary, the interior nodes of the mesh move but their connectivity does not change. This ensures mesh conservation [17].

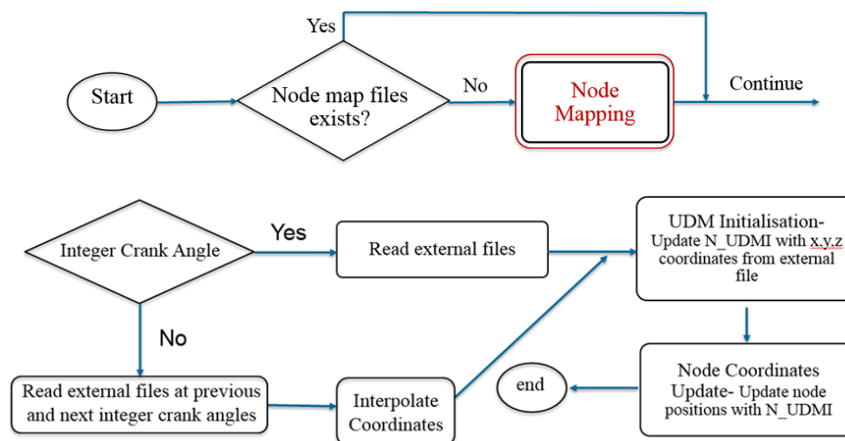


**Figure 1.** Flow chart of User Defined Functions to link SCORG with FLUENT

The above flow chart (Figure 1) has been modified for it to adapt with the parallel solver in comparison to similar flow chart developed for numerical simulations in sliding vane rotary machines [16]. Node coordinates update occurs using User Defined Node Memories (UDNMs), which are memory locations defined for every node that need to be initialized before hooking the UDF. Once nodes are mapped (explained in section 3.2), a first UDNM is initialised with the mapping index corresponding to the each node. Afterwards, at each time step, the corresponding grid data file is read and unmapped node coordinates are stored in auxiliary matrixes. Three additional UDNMs are used to store mapped X, Y, Z coordinates of each node respectively. A cell loop eventually assigns UDNMs values to node coordinates. If a solver exit operation is performed, the next restart automatically picks up the right node file calculated using the flow time in the data file and calculations can continue without disruption. Depending on the angular step set in the grid generation, the number of mesh files per revolution changes. Eventually, UDNMs are initialised with calculated node coordinates.

SCORG grid files are generated with an angular step change and this angular step change is dependent on number of rotor grid files per revolution. If the exact rotor grid files are not available according to the angular step change then linear interpolation of node coordinates is performed in the UDF. Extension of above flow chart with parallelisation is discussed in section below.

### 3. Parallelisation

#### 3.1 Parallel Architecture

Parallel computing techniques have been very well developed in the past two decades which brought in emergence of faster networks, massive distributed systems, and multi-processor or multi-core computer architectures even at the desktop level. CFD solvers are Finite Volume Method (FVM), the parallelisation is based on domain decomposition approach by which the full computational domain is partitioned into sub-domains. Calculations or tasks occur at each sub-domain as it is assigned to a processor.

CFD solver parallelisation is typically data parallelisation which is focused on distributing computer nodes with the processors with them responsible to execute the same algorithm. FLUENT uses Message Passing Interface (MPI) which in parallel computing terms are standard and reliable set of libraries that are used for communicating information between the different processors, cores or even computers. Along with MPI, FLUENT uses additional node or host processors with its own terminology named 'host' to take care of I/O operations and interact with other user output. Host nodes and the computer node 0, both physically reside on the same computer node. In this case, multiple processes are executed on the same machine. Figure 2(b) shows simple case of partitioned mesh in parallel FLUENT [17]. When the mesh is partitioned it should be ensured single copy of nodes is maintained.

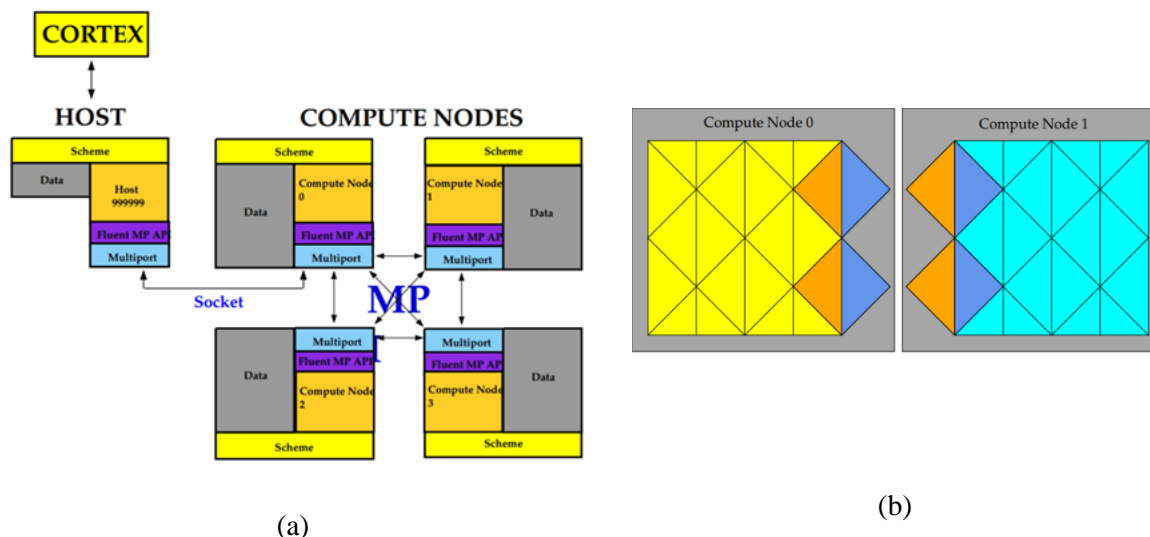


**Figure 2.** (a) Parallel FLUENT architecture (b) Partitioned mesh distributed between two computer nodes [17]

FLUENT has a set architecture through to perform calculations and data transfer (Figure 2(b)). Cortex sends commands to the host which in turn passes the command to Node-0. Node-0 does not perform any operation apart from displaying messages and passing data. Node-0 passes messages to Node-1 to Node-n to process data and this data when processed is sent back to Node-0. Each computer node is virtually connected to each other computer node and relies on its communicator to perform functions on sending or receiving arrays, synchronising and establishing machine connectivity [17].

#### 3.2 UDF Parallelisation

As mentioned in the previous section that node mapping is computationally intensive and therefore it needs to be parallelised as the almost all CFD simulations are almost solved with a parallel solver. If node is not parallelised and used with a parallel solver it will simply lead to node duplication with resulting error and mismatch of nodal information.

Text files with information on node numbers and rotor co-ordinates are written from SCORG™ and these are numbered according to angular rotor positions. Node mapping uses the first rotor position file

‘rotor.1’, this file is processed in HOST. Node coordinates from this file is assigned to an array and passed on to the other computer nodes. Node number between input data file and mesh loaded in FLUENT are different as shown in Figure 3 and this trend is seen three dimensionally. The mapping criteria is based on the minimum distance between the nodes in the FLUENT mesh and data file (Equation 1). Distance is computed on the different computer nodes according to the equation below. Where j represents nodes from FLUENT mesh, i represents nodes from data file at first time step and x,y,z represent node coordinates. Once the distance is computed, then every node distance is compared with each other through a loop and minimum distance is found. The ID of node with minimum distance is then stored in user-defined memory in mesh node (N\_UDMI(0)). Information from all the mesh nodes is transferred by to computer Node 0 and Node 0 receives the data in synchronised manner which is then transferred to the HOST. HOST simply receives the data and writes in to a .txt file.

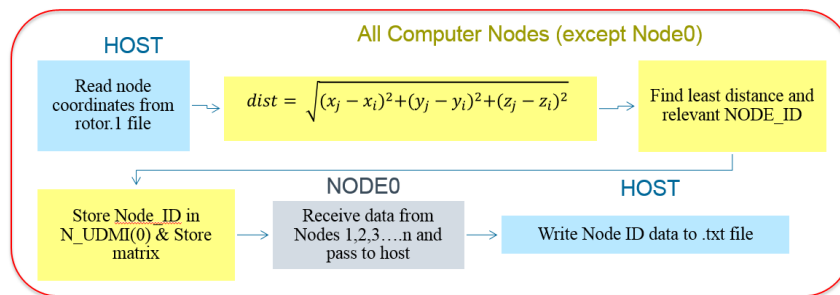


**Figure 3.** Flow chart for node mapping with parallel architecture

$$distance = \sqrt{(x_j - x_i)^2 + (y_j - y_i)^2 + (z_j - z_i)^2} \tag{1}$$

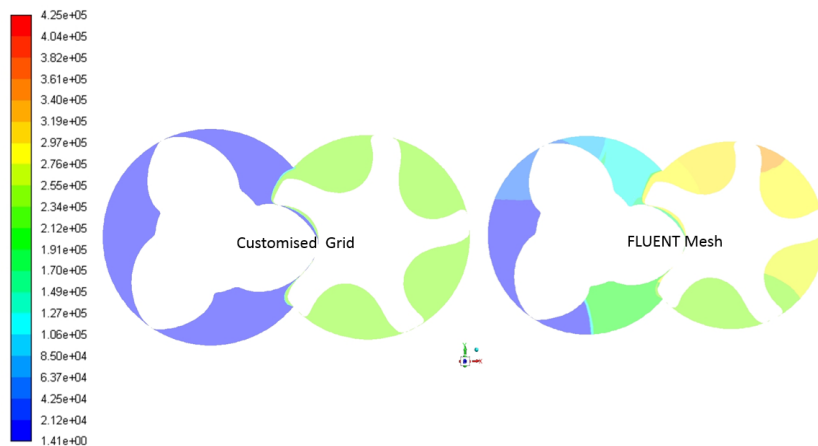


**Figure 4.** Node number mismatching between mesh loaded in FLUENT and customised grid generated by SCORG

**Table 1.** Comparison between time taken between serial and parallel solver for node mapping

| Case No. | No. of domain nodes | Serial         | Parallel       |                | Improvement in time (%) |
|----------|---------------------|----------------|----------------|----------------|-------------------------|
|          |                     | Time taken (s) | Computer nodes | Time taken (s) |                         |
| Case 1   | 11,640              | ~100           | 4              | 20-25          | 300-400%                |
| Case 2   | 58,850              | 580            | 4              | 140            | 315%                    |
| Case 3   | 523,867             | 41400          | 4              | 11020          | 325%                    |

Figure 4 shows difference in mismatch in node number between mesh loaded in FLUENT and original grids generated in SCORG. Table 1 provides a brief summary of cases with different cell node numbers being mapped in serial as well as parallel solver and compared with each other for improvement in time. All the computer nodes are taken as four to provide a consistent way of comparing and it can be seen that the improvement in time when a parallel solver of 4 nodes is used is around 330%.

#### 4. Test Case

Compressor used for this study is an oil-free twin screw compressor with a 3/5 lobe arrangement and 'N' rotor profile rotors. The operating speed on the male rotor tested for this study is 6000 RPM and 8000 RPM. The male rotor diameter is 127.45 mm; the female rotor diameter is 120.02 mm while the centre distance between the two rotors is 93.00 mm. The length to diameter ratio of the rotors is 1.6, male rotor has a wrap angle 285.0 deg and the built-in volume index of 1.8.

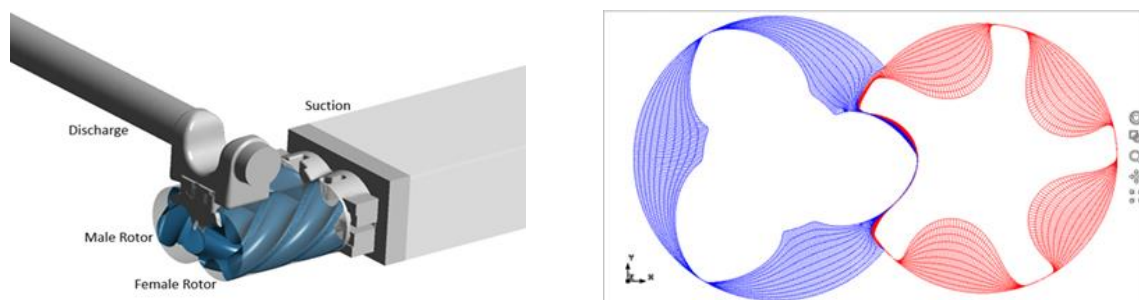


**Figure 5.** Left: Extracted computation fluid domain and Right: Grid distribution in SCORG for first rotor position

Figure 5 Left shows fluid domain. Measurements related this compressor has been documented in previous literatures [12]. Uniform radial and interlobe clearances of 60  $\mu\text{m}$  are used in this study and end leakage is considered to account for axial clearance of 100  $\mu\text{m}$ . The working fluid is air. A molar mass of 28.96 kg/kmol, specific heat capacity 1004.4 J/kg K, dynamic viscosity  $1.831 \times 10^{-5}$  kg/m s and thermal conductivity 2.61e-02 W/m K. A uniform pressure of 1.0bar was specified at the suction while discharge pressure of 2.0bar was analysed for speeds of 6000 RPM and 8000 RPM.

The deforming rotor domain is meshed with an external grid generator software called SCORG. Figure 5 Right, shows single domain conformal grids for first position of the male rotor. For grid, radial divisions is 10, angular divisions is 50, interlobe divisions is 50 which gives total circumferential divisions of 350. Same grids generated from SCORG are used for both CFX and FLUENT solver to make a good comparison with the predicted results.

##### 4.1 Solver

Both CFX and FLUENT are finite-volume method solvers while CFX is vertex-centred solver and FLUENT is cell-centred solver. In the cell-centered approach, mesh generated from SCORG<sup>TM</sup> serves as a control volume and the average variable value is stored in its center. On the other hand, for the vertex-centered method; the spatial domain is firstly discretised into a mesh by using an external grid generator like SCORG<sup>TM</sup>. This mesh is then used to construct virtual control volumes within the solver. One important advantage of the cell-centered method is its capability of computing fluxes in nonconforming cell interfaces where the vertex-centered method is not equally flexible and requires expensive procedure to compute the fluxes.

In segregated solver, the governing equations are solved separately. First, momentum equations are solved using the updated values of pressure and face mass fluxes and this followed by pressure correction equation. Face mass fluxes, pressure, and the velocity field are then corrected using the pressure correction obtained from a pressure-velocity coupling solution. The solution is run iteratively until the convergence criteria is met. In FLUENT, algorithms developed for P-V coupling for segregated



solver are SIMPLE, SIMPLEC and PISO. Also, a coupled scheme is available which is based on pressure-based coupled solver. In coupled approach, system of momentum equations and the pressure-based continuity equation is solved in one step. The remaining equations, such as energy and turbulence, are solved in a decoupled manner. It is expected that memory requirements with coupled solver are higher compared to a segregated solver since the momentum and pressure-based continuity equations need to be stored in the memory at the same time.

#### 4.2 Numerical Set-up

Numerical setup selections with CFX and FLUENT are shown in Table 2. Most of numerical selections for both the solvers are chosen to be same apart from turbulence model, but both the models are Reynolds Averaged Navier-Stokes turbulence models. It can be noticed that FLUENT requires more number of iterations to approach converged solution with deforming grids compared to CFX. In spite of higher inner coefficients loop with FLUENT, the required calculation time is three times lower than CFX. This again proves that SIMPLE algorithm is faster compared to coupled algorithm (Table 3). Also, the averaged mass imbalance for both the solvers is quite solver with a small difference of 2%.

**Table 2.** Numerical setup used for FLUENT and CFX solver

| Criteria                          | Selection- CFX                               | Selection- FLUENT                             |
|-----------------------------------|--|---|
| Turbulence Model                  | SST- k Omega                                 | k-epsilon                                     |
| Inlet Boundary Condition          | Opening (specified pressure and temperature) | Inlet (specified pressure and temperature)    |
| Outlet Boundary Condition         | Opening (with specified temperature )        | Pressure outlet (with specified temperature ) |
| Pressure-Velocity Coupling        | Co-located layout                            | SIMPLE (first order upwind)                   |
| Turbulence Scheme                 | First order upwind                           | First order upwind                            |
| Transient Scheme                  | First order upwind                           | First order implicit                          |
| Transient Inner loop coefficients | Up to 10 iterations per time step            | 30 iterations per time step                   |
| Convergence Criteria              | 1e-03  | 1e-03   |
| Relaxation parameters             | 0.1  | 0.1   |

**Table 3.** Solution time with FLUENT and CFX solver

| Solver | Calculation time/time step/core | Error in cycle averaged mass flow |
|--------|---------------------------------|-----------------------------------|
| CFX    | 7.30 mins                       | 1.01                              |
| FLUENT | 2.40 mins                       | 0.99                              |

## 5. Results and discussion

This section explores the results obtained by CFD solution in the form of variation in pressure within compression chamber, flow velocity, volume flow rate, indicated power and specific power of the compressor.

### 5.1 Pressure-angle diagram

Figure 6 shows the variation of chamber pressure with the male rotor rotation angle for speeds 8000 RPM and 6000 RPM. In this figure, comparison is made between absolute pressure obtained by

FLUENT and CFX over a compression cycle against experimentally obtained data. The pressure calculated by both the solvers agrees well with the experimental data. Slight differences are noticed at peak pressure where pressure predicted by FLUENT solver is closer to experiments compared to CFX solver. It might have been expected that coupled scheme used with CFX would have better predicted peak pressure as in coupled algorithm pressure based continuity equation is solved rather than guessed and corrected using pressure correction equation. However, one is cell centred and other is vertex centred solver where pressure has higher number of approximations due a number of vertices present within the cell [18]. This might have led to lower prediction of peak pressure with CFX compared to experiments

Additionally, throttling of pressure at discharge is not seen with FLUENT solver for 8000 RPM this might be due to nature of boundary condition used with FLUENT which is 'pressure outlet'. With 'pressure outlet' backflow is not obtained. This was corrected with later version of ANSYS 19.0 for the case with male rotor speed of 6000 RPM and due to some amount of backflow is in Figure 6 Right.

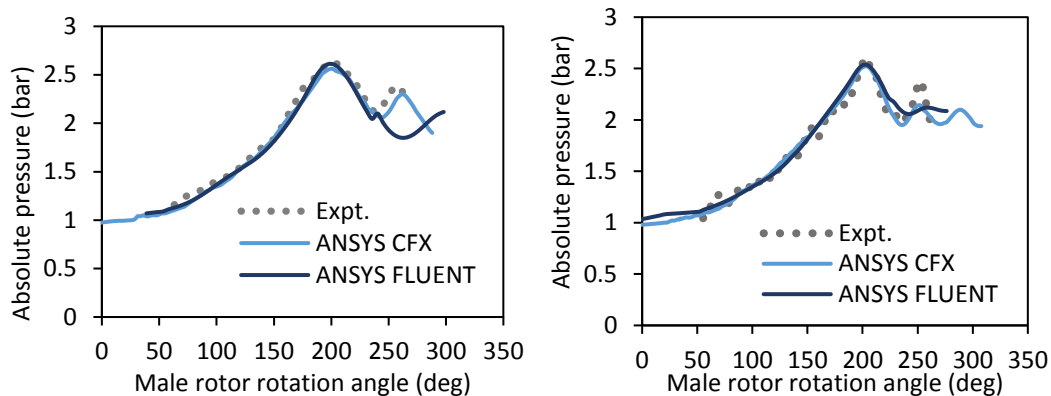


**Figure 6.** Pressure-angle comparison at 2.0 discharge bar for Left: 8000 RPM and Right: 6000 RPM

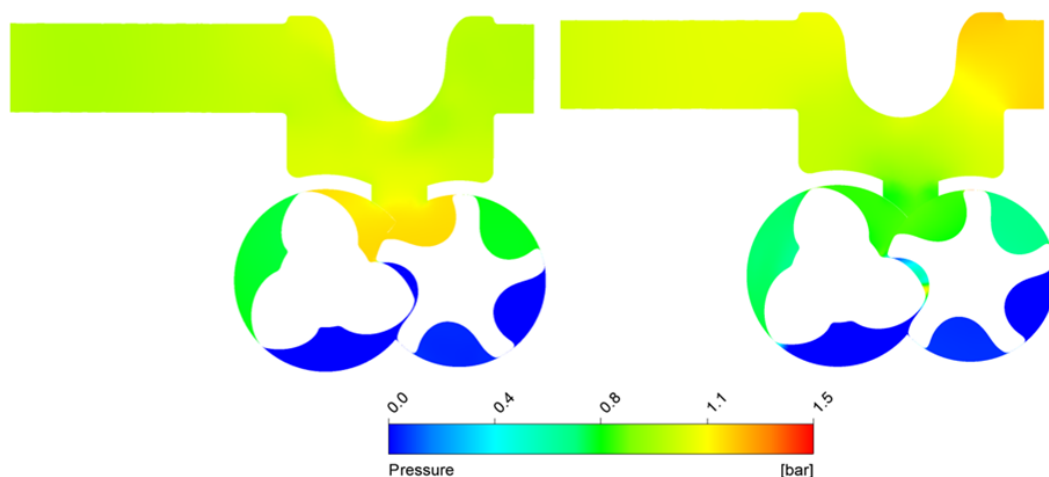


**Figure 7.** Gauge pressure contour plot Left: CFX and Right: FLUENT at cross-section  $z=0.182$  m and time step= 852 for male rotor speed of 8000 RPM

Figure 7 shows the pressure contours obtained at cross section ( $z = 0.182$  m) for male rotor speed at 8000 RPM, both the contour plots show similar pressure characteristics at the cross section. Comparatively lower pressure is seen near the discharge side of rotors with Fluent and higher pressure gradient is seen in the inter-lobe region.

### 5.2 Flow rate

It can be clearly seen that FLUENT predicts flow rate closer to experimental data with an error percentage of 8.5% whereas CFX predicts flow rate with error percentage of 13.5% for male rotor speed of 8000 RPM. For 6000 RPM, error in flow rate prediction with CFX is 7% and with FLUENT is 3.4%. Although the clearances in rotor domain vary during operation from one region to another, but in CFD the average clearances are specified as fixed throughout the compressor operating condition. This might introduce some inaccuracies.

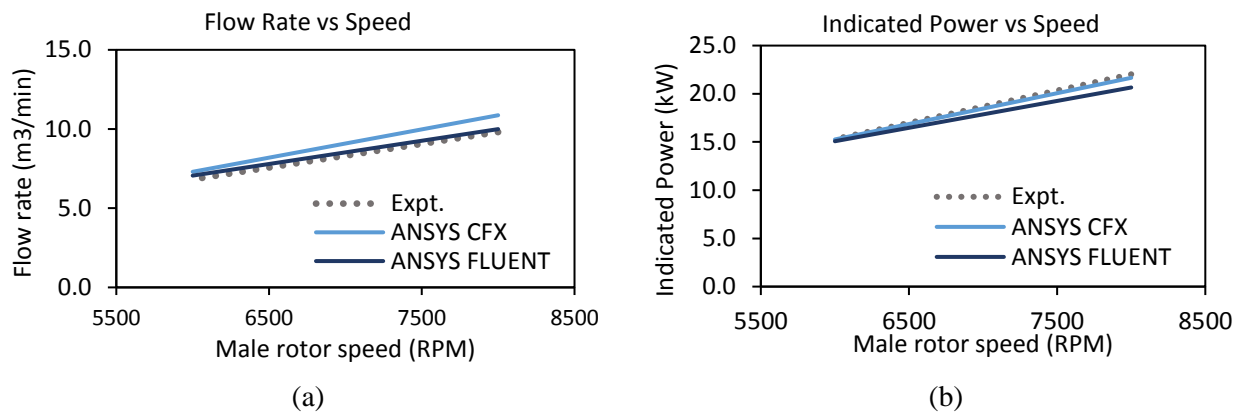


**Figure 8.** Comparison of experimental data and CFD predictions for (a) flow rate (b) indicated power

### 5.3 Power

In the experiment, the power was measured on the motor shaft and a constant mechanical efficiency of 95% was assumed for the integral gearbox at all speeds. Figure 8b shows the comparison of indicated power predicted from CFD calculations with experimental data. CFX predicts indicated power with an error of 1.7% whereas FLUENT predicts indicated power with an error of 6.2%. This might be due to the boundary condition of outlet type used with FLUENT where there is no backflow allowed. When the backflow is allowed with newer version of FLUENT 19.0 for case with 6000 RPM, higher predictions of indicated power are seen 1.5% whilst CFX predicts with error percentage of 0.3%. Though higher error percentage of power is seen with FLUENT when compared with experiments, but these experimental measurement contain power related to mechanical losses. This is not calculated in CFD, which means the power predictions with FLUENT are better than CFX.

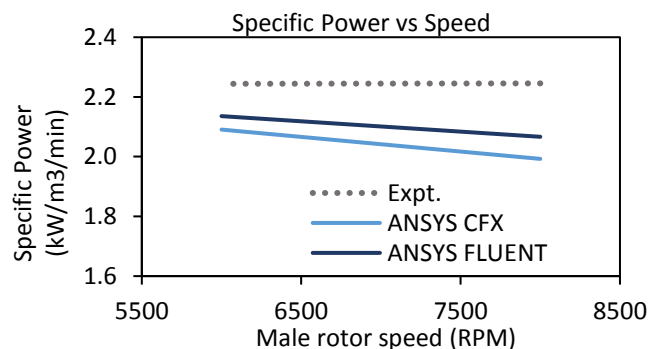


**Figure 9.** Comparison of experimental data and CFD predictions for specific power

Specific power is the ratio of the indicated power and flow through the compressor. A lower specific power indicates a better machine. Figure 9 compares the specific power prediction from the CFD calculations for FLUENT and CFX with the experimental data. There is very slight difference in error percentage of around 0.1% with FLUENT predicting better than CFX.

## 6. Conclusion & future work

Oil free twin screw air compressor is modelled in FLUENT (segregated approach) by using an interface with customised grid generator SCORG™. This interface comprises of UDND for smooth movement of interior nodes in an extended parallel framework. The developed setup is tested for an industrial air compressor with the discharge pressure of 2 bar and male rotor shaft speeds of 6000 RPM and 8000 RPM

- Extension of UDND code for parallel computation has led to faster mapping of nodes with linear improvement in time
- This study has demonstrated that the segregated algorithm in FLUENT is three times faster than the coupled CFX solver for the same case
- FLUENT had predicted better flow rate than CFX for both 8000 RPM and 6000 RPM whilst indicated power predicted by CFX is closer to experimental data. However, experimental data includes power due to mechanical losses which are not predicted through CFD and this in respect predictions from FLUENT are better than CFX

This study provides a strong basis to extend the current setup to solve for an oil-injected compressor with Eulerian-Eulerian multiphase flow model. Developed parallelisation interface and segregated algorithm with FLUENT will be helpful as computational time required for multiphase flows is significantly higher than for the single phase.

## References

- [1] P. Radgen and E. Blaustein, *Compressed Air Systems in the European Union Energy, Emissions, Savings Potential and Policy Actions*. 2001.
- [2] “Improving Compressed Air System Performance: A Sourcebook for Industry,” *Compressed air challenge (CAC)*, 2011.
- [3] I. A. Sakun, *Vintovie kompresorii (Screw Compressors)*. Mashinostroenie Leningrad, 1960.
- [4] N. Stosic, I. Smith, A. Kovacevic, and E. Mujic, “Three Decades of Modern Practice in Screw Compressors,” in *International Compressor Engineering Conference*, 2010.
- [5] “Screw Compressor Market 2017 - Global Forecast to 2021: Market to Grow at CAGR of 6.62% to reach \$11 Billion - Research and Markets,” *Research and Markets*, Dublin, 26-Jan-2017.
- [6] K. Hanjalic and N. Stosic, “Development and Optimization of Screw Machines With a Simulation Model—Part II: Thermodynamic Performance Simulation and Design Optimization,” *Journal of Fluids Engineering*, vol. 119, no. 3, pp. 664–670, 1997.
- [7] N. Stošić, L. Milutinović, K. Hanjalić, and A. Kovačević, “Investigation of the influence of oil injection upon the screw compressor working process,” *International Journal of Refrigeration*, vol. 15, no. 4, pp. 206–220, 1992.
- [8] A. Kovacevic, “Three-Dimensional Numerical Analysis for Flow Prediction in Positive Displacement Screw Machines,” City University London, 2002.
- [9] A. Kovacevic, “Boundary adaptation in grid generation for CFD analysis of screw compressors,” *International Journal for Numerical Methods in Engineering*, vol. 64, no. 3, pp. 401–426, 2005.
- [10] A. Kovacevic, N. Stosic, and I. Smith, *Screw Compressors: Three Dimensional Computational Fluid Dynamics and Solid Fluid Interaction*. Springer Verlag, Berlin, 2005.
- [11] S. Rane and A. Kovacevic, “Advances in Engineering Software Algebraic generation of single domain computational grid for twin screw machines . Part I . Implementation,” *Advances in Engineering Software*, vol. 107, pp. 38–50, 2017.
- [12] A. Kovacevic and S. Rane, “Algebraic generation of single domain computational grid for twin

- screw machines Part II Validation, *Advances in Engineering Software*, 2017.
- [13] A. Kovacevic, S. Rane, and N. Stosic, “Computational Fluid Dynamics in Rotary Positive Displacement Screw Machines,” in *ISROMAC2016*, 2016.
- [14] N. Casari, M. Pinelli, A. Suman, and D. Ziviani, “Full 3D numerical analysis of a twin screw compressor by employing open-source software.”
- [15] A. Kovacevic, S. Rane, and N. Stosic, “Modelling of Multiphase Twin Screw Machines,” in *New Technologies, Development and Applications*, 2019, no. September 2018.
- [16] G. Bianchi, S. Rane, A. Kovacevic, and R. Cipollone, “Deforming grid generation for numerical simulations of fluid dynamics in sliding vane rotary machines,” *Advances in Engineering Software*, vol. 112, pp. 180–191, 2017.
- [17] “ANSYS FLUENT 12.0 UDF Manual,” 2010.
- [18] H. Hægland, A. Assteerawatt, H. K. Dahle, G. T. Eigestad, and R. Helmig, “Comparison of cell- and vertex-centered discretization methods for flow in a two-dimensional discrete-fracture-matrix system,” *Advances in Water Resources*, vol. 32, no. 12, pp. 1740–1755, 2009.